



# THE MAGNETIC FORM FACTORS FOR SOME NUCLEI $^{51}\text{V}$ , $^{59}\text{Co}$ , $^{93}\text{Nb}$ , $^{115}\text{In}$ BY USING VALENCE WITH AND WITHOUT CORE POLARIZATION EFFECTS MODELS<sup>†</sup>

 Sajad A. Khasain\*,  Khalid S. Jassim

*Department of Physics, College of Education for Pure Sciences, University of Babylon, 51002 Babylon, Iraq*

*\*E-mail: [sajad.ali.pure304@student.uobabylon.edu.iq](mailto:sajad.ali.pure304@student.uobabylon.edu.iq)*

Received March 3, 2023; revised May 07, 2023; accepted May 08, 2023

The magnetic electron scattering form factor with *glekpn*, *d3f7*, *ho* models space for  $^{51}\text{V}$ ,  $^{59}\text{Co}$ ,  $^{93}\text{Nb}$ , and  $^{115}\text{In}$  nuclei are discussed with and without core polarization effects (CP). The calculations are done with the help of NuShellX@MUS code. The radial wave function for the single-particle matrix elements have been calculated with the Skyrme-Hartree Fock (SKX), Wood–Saxon (WS), and harmonic oscillator (HO) potentials. valence model (Vm) used in these calculation to calculate form factors with core-polarization effects. The results give a good agreement with available experimental data.

**Keywords:** *electron scattering; transverse form factor*

**PACS:** 25.30.Bf, 21.10.Ft, 25.30Dh

## 1. INTRODUCTION

A special method for examining the electromagnetic characteristics of nuclei and learning about their charge and current distributions is electron scattering. Several reasons for using electrons as probes. The electromagnetic force, the most well-known interaction and one that quantum electrodynamics (QED) fully describes, is what first causes the electron to interact with the nucleus. Additionally, the interaction's coupling constant is not strong enough to materially alter the nuclear structure under investigation. Additionally, one may operate in first order perturbation inside the one-photon exchange approximation due to the interaction's weakness. Second, unlike with actual photons, the energy transfer and momentum transfer may be changed separately, allowing for the mapping of the densities' Fourier transform. Past research on electron scattering in the elastic, inelastic, and quasi-elastic regimes has produced the most precise measurements of charge radii, transition probabilities, momentum distributions, and spectroscopic parameters [1].

The nuclear shell model has shown to be a highly useful tool for studying nuclear structure because it can accurately and systematically account for many observable by choosing the right residual effective interaction. The creation of a nuclear shell model has advanced the understanding of nuclear structure. The shell model, while fundamentally simple, describes a variety of nuclear phenomena, including spin, magnetic moment, and nuclear spectra [2].

One of these models, the shell model with a constrained model space (MS), when effective charges are utilized, is successful in characterizing the static characteristics of nuclei. The core orbits are deformed in a manner that is compatible with the quadrupling of the valance orbits [3].

The aim of this study is to investigate electron scattering form factors that constitute the inelastic transverse electron scattering of  $^{51}\text{V}$ ,  $^{59}\text{Co}$ ,  $^{93}\text{Nb}$  and  $^{115}\text{In}$ . In these calculations, the nucleation model in the fp-shell and g-shell regions. The coincidence model calculations will be performed using the interaction of *w0*, *ho* and *glekpn* (constraint) effective for the fp and gf model space. The shell model calculation will be performed using NuShellX@MSU [4]. The Valence + core polarization (Vm+CP) and valence models (Vm) only uses the appropriate efficiencies for the neutron and proton inelastic form factors were calculated. Our theoretical results will be compared with previously collected experimental data. Electron scattering form factors of some nuclei have been studied by Jassim and et. al. [5]. Li, Xin and et.al. have been made comparative studies on nuclear elastic magnetic form factors between the relativistic and non-relativistic mean-field approaches [6].

## 2. THEORY

The formalism of electron scattering from deformed nuclei that we follow in this work. All nuclear information is included in the longitudinal form factor  $F_L(q)$ , which represents scattering from the nuclear charge density, and the transverse form factor  $F_T(q)$ , which represents scattering from the nuclear current density

<sup>†</sup> *Cite as:* S.A. Khasain, K.S. Jassim, East Eur. J. Phys. 2, 317 (2023), <https://doi.org/10.26565/2312-4334-2023-2-36>

© S.A. Khasain, K.S. Jassim, 2023

structural details [7]. The differential cross-section for electron scattering from a nucleus with mass (M) and charge (Ze) into angle (d) in PWBA ( plane-wave Born approximation) is given by [8]:

$$\frac{d\sigma}{d\Omega} = \left(\frac{d\sigma}{d\Omega}\right)_{Mott} f_{rec} \sum_J |F_J(q, \theta)|^2, \tag{1}$$

where the cross-section of the Mott is represented by  $\left(\frac{d\sigma}{d\Omega}\right)_{Mott}$ . The scattering of a relativistic electron from a spin-free point charge at high energy is given by [9]:

$$\left(\frac{d\sigma}{d\Omega}\right)_{Mott} = \left(\frac{Ze^2 \cos\left(\frac{\theta}{2}\right)}{2E_i hc \sin^2\left(\frac{\theta}{2}\right)}\right)^2. \tag{2}$$

It is known as the nuclear recoil factor:

$$f_{rec} = \left(1 + \frac{2E_i}{M} \sin^2\left(\frac{\theta}{2}\right)\right)^{-1} \tag{3}$$

The total form factor  $F_J(q, \theta)$  of a certain multi-polarity is described as having a transverse part  $F_J^T(q)$  and a Longitudinal (Coulomb) part  $F_J^L(q)$  and is defined as [10]:

$$F_J^2(q, \theta) = \left(\frac{q_u}{q}\right)^4 |F_J^L(q)|^2 + \left[\frac{q_u^2}{2q^2} + \tan^2\left(\frac{\theta}{2}\right)\right] |F_J^T(q)|^2, \tag{4}$$

where  $q_u$  stands for the four momentum transfer, q stands for momentum transfer and  $\theta$  stands for the scattering angle. It is possible to express the effective momentum transfer by  $q_{eff}$  can be written as [11]:

$$q_{eff} = q \left[1 + \frac{3}{2} \frac{Ze^2}{E_i R_c}\right], \tag{5}$$

where  $R_c = \sqrt{\frac{5}{3}} r_{rms}$ .

Parity and time reversal invariance indicate that only the even and odd transverse magnetic multipoles contribute to elastic scattering. Then, in PWBA, only odd magnetic multipoles will remain after  $\theta = 180$ .

$$|F_T(q)|^2 = \sum_{\lambda=odd} |F^{M\lambda}|^2 \tag{6}$$

The definition of the magnetic multi pole operators is

$$\hat{T}_\mu^{M\lambda}(q) =_{i\lambda} \int dr j_\lambda(qr) Y_{\lambda\lambda}^\mu(\Omega_r) \cdot \hat{J}(r), \tag{7}$$

where the operator for current density is  $\hat{J}(r)$ . The convection and magnetization components of the currents  $\hat{J}$  in the transverse form factors result from the motion and intrinsic magnetic moments of the nucleons, respectively. We adjust for the center of mass (c.m.) and finite nucleon sizes when calculating the overall form factors. The common factor produced from the harmonic-oscillator approximation is used for the c.m. correction.

$$F_{c.m}(q) = \exp(q^2 b^2 / 4A), \tag{8}$$

where A is the mass number of the nucleus and b is the harmonic oscillator size parameter [1].

With isospin, the form factor adopts the form

$$F_J^2(q) = \frac{4\pi}{Z^2(2J_i + 1)} \sum_{T=0,1} (-1)^{T_f - T_i} \begin{vmatrix} T_f & T & T_i \\ -T_Z & 0 & T_Z \end{vmatrix}, \tag{9}$$

$$|\langle J_f T_f || \hat{L}_{JT}(q) || J_i \rangle|^2 |F_{c.m}(q)|^2 |F_{f.s}(q)|^2.$$

Where  $F_{f.s}(q)$  is the finite size correction given by

$$F_{f.s}(q) = \exp(-0.43q^2/4). \tag{10}$$

Where  $T_Z = \frac{Z-N}{2}$  and T given by:

$$|T_i - T_f| \leq T \leq T_i + T_f, \tag{11}$$

see [12].

### 3. RESULT AND DISCUSSION

The nuclei under examination have 11 and 19 particles outside the core  $^{40}\text{Ca}$  for  $^{51}\text{V}$  and  $^{59}\text{Co}$ , and 37,59 particles outside the core  $^{56}\text{Ni}$  (with restriction usade) for  $^{93}\text{Nb}$  and  $^{115}\text{In}$  respectively. Calculations using Valence model with and without core-polarization effects. NuShellX@MUS was used for all calculations with the SKx, WS, HO potential.

#### 3.1. Magnetic form factor for $^{51}\text{V}$

The transverse form factor calculations have been performed in the d3f7 model space with the shell-model code NUSHELLX X@MUS since we are interested in the negative-parity states of  $^{51}\text{V}$  for the valance particles states outside the core  $^{40}\text{Ca}$ , The  $V_m(a)$  and the  $V_m$  with CP model (b) are compared in the (Figure 1) as the total magnetic form factor which symbolizes the sum.

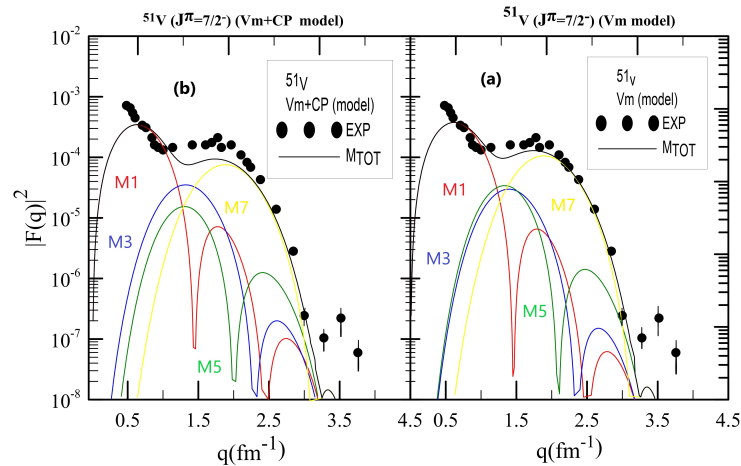


**Figure 1.** The transverse magnetic form factor for  $^{51}\text{V}$  ( $J^\pi = \frac{7}{2}^-$ ). The experiment's findings are based on Ref [12], [13], [14].

The contribution of M1, M3, M5, and M7 for  $^{51}\text{V}$  ( $J^\pi = \frac{7}{2}^-$ ) is shown in red, blue, green, and yellow, respectively. Effective interaction (W0). It was applied to the fp-shell model space wave function. In the first peak between  $(0 \leq q \leq 1.5)\text{fm}^{-1}$ , the dominant component is M1 where the maximum values are  $10^{-3}$  and  $(0.6)\text{fm}^{-1}$  for form factors and momentum transfer values respectively. At the second peak between  $(1.5 \leq q \leq 3)\text{fm}^{-1}$ , the dominant component is M7 where the maximum values are  $10^{-4}$  and  $(3)\text{fm}^{-1}$  for form factors and momentum transfer values respectively, There is no rapprochement between the experiment's and the theoretical data for the final peak.

Figure (2) compares the total magnetic form factor between the Valence model( $V_m$ )shown in red line and the Valence model with core polarization ( $V_m+CP$ ) shown in blue line It is clear from the peaks in the figure that the core effect is very small, because the form factor in our work is transverse.

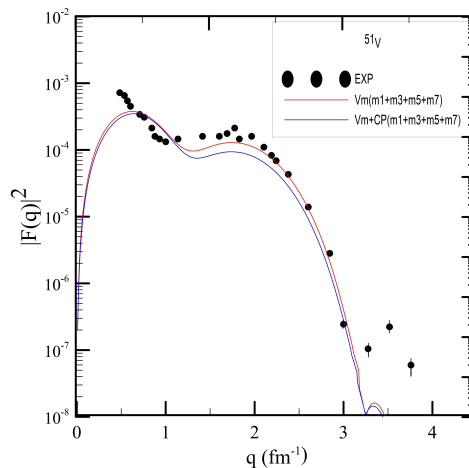


**Figure 2.** Demonstrates compare between  $V_m$  and  $V_m+CP$  models for  $^{51}\text{V}$  ( $J^\pi = \frac{7}{2}^-$ ).

### 3.2. Magnetic form factor $^{59}\text{Co}$

The transverse form factor calculations have been performed in the model space ( $ho$ ) since we are interested in the negative-parity states of  $^{59}\text{Co}$  for the valance particles states outside the core  $^{40}\text{Ca}$ , The  $V_m(a)$  and the  $V_m$  with CP model ( $b$ ) are compared as the total magnetic form factor, which symbolizes the sum. The contribution of M1, M3, M5, and M7 for  $^{59}\text{Co}$  ( $J^\pi = \frac{7}{2}^-$ ) is shown in red, blue, green, and yellow, respectively. Effective interaction ( $ho$ ). It was applied to the fp-shell model space wave function. In the first peak between  $(0 \leq q \leq 1.3)fm^{-1}$ , the dominant component is M1 where the maximum values are  $10^{-3}$  and  $(0.7)fm^{-1}$  for form factors and momentum transfer values respectively. At the second peak between  $(1.5 \leq q \leq 3.4)fm^{-1}$ , the dominant component is M7 where the maximum values is  $10^{-4}$  and  $(2.3)fm^{-1}$  for form factors and momentum transfer values respectively.

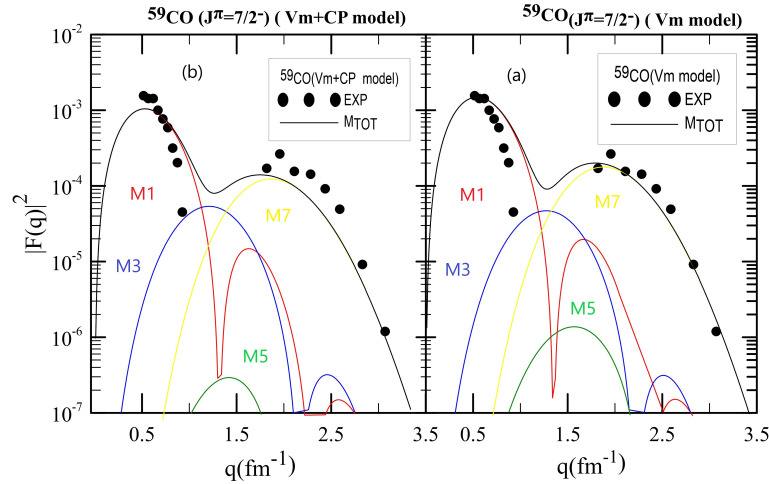


**Figure 3.** The transverse magnetic form factor for  $^{59}\text{Co}$  ( $J^\pi = \frac{7}{2}^-$ ). The experiment's findings are based on Reference[12],[15][16].

Figure (4) compares the total magnetic form factor between the Valence model ( $V_m$ ), shown in red line, and the Valence model with core polarization ( $V_m+CP$ ), shown in blue line. It is clear from the peaks in the figure that the core effect is very small, because the form factor in our work is transverse.

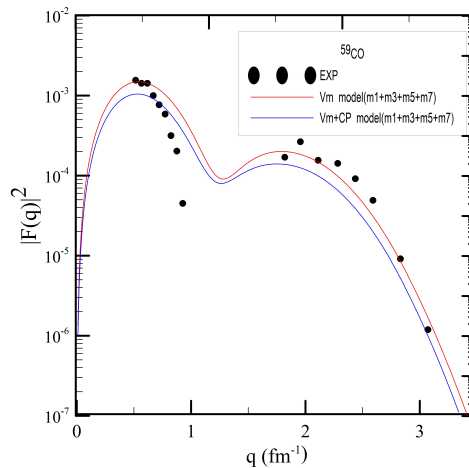


**Figure 4.** Demonstrates compare between  $V_m$  and  $V_m+CP$  models for  $^{59}\text{Co}(J^\pi = \frac{7}{2}^-)$ .

### 3.3. Magnetic form factor $^{93}\text{Nb}$

The transverse form factor calculations (Figure 5) have been performed in the ( $glekpn$  with restriction) model space with the shell-model code NUSHELL X@MUS since we are interested in the positive-parity states of  $^{93}\text{Nb}$  for the valance particles states ( $1g7/2$ ) outside the core  $^{56}\text{Ni}$ , The  $V_m$  ( $a$ ) and the  $V_m$  with CP model ( $b$ ) are compared as the total magnetic form factor, which symbolizes the sum. The contribution of M1, M3, M5, and M7 for  $^{93}\text{Nb}$  ( $J^\pi = \frac{9}{2}^+$ ) is shown in red, blue, green, and yellow, respectively. Effective interaction  $glekpn$ .

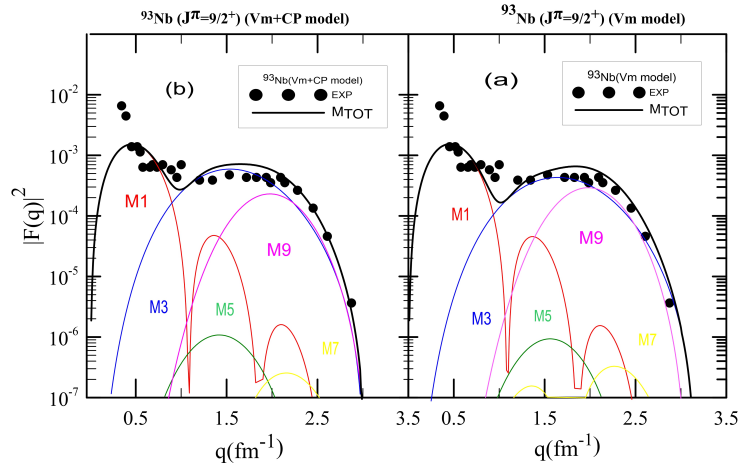


**Figure 5.** The transverse magnetic form factor for  $^{93}\text{Nb}(J^\pi = \frac{9}{2}^+)$ . The experiment's findings are based on Reference [12][17][15].

It was applied to the g-shell model space wave function. In the first peak between  $(0 \leq q \leq 1.1)\text{fm}^{-1}$ , the dominant component is M1 where the maximum values are  $10^{-3}$  and  $(0.6)\text{fm}^{-1}$  for form factors and momentum transfer values respectively. At the second peak between  $(1.4 \leq q \leq 3)\text{fm}^{-1}$ , the dominant component is M3 where the maximum values are  $10^{-3}$  and  $(1.7)\text{fm}^{-1}$  for form factors and momentum transfer values respectively.

Figure (6) compares the total magnetic form factor between the Valence model (Vm), shown in red line, and the Valence model with core polarization (Vm+Cp), shown in blue line. It is clear from the peaks in the figure that the core effect is very small, because the form factor in our work is transverse.

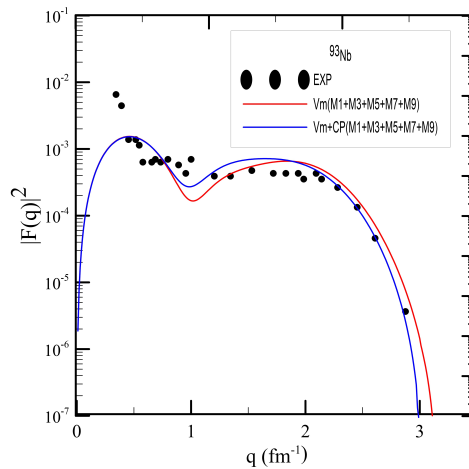


**Figure 6.** Demonstrates compare between Vm and Vm+CP models for  $^{93}\text{Nb}(J^\pi = \frac{9}{2}^+)$ .

### 3.5. Magnetic form factors of $^{115}\text{In}$

The transverse form factor calculations Figure (7) have been performed in the (*glekpn* whit restriction) model space since we are interested in the positive-parity states of  $^{115}\text{In}$  for the valance particles states  $(1g7/2)$  outside the core  $^{56}\text{Ni}$ . The Vm (a) and the Vm with CP model (b) are compared as the total magnetic form factor, which symbolizes the sum. The contribution of M1, M3, M5, and M7 for  $^{115}\text{In}(J^\pi = \frac{9}{2}^+)$  is shown in red, blue, green, and yellow, respectively. Effective interaction *glekpn*. It was applied to the g-shell model space wave function. In the first peak between  $(0 \leq q \leq 1)\text{fm}^{-1}$ , the dominant component is M1 where the maximum values are  $10^{-3}$  and  $0.5\text{fm}^{-1}$  for form factors and momentum transfer values respectively. At the second peak between  $(1.6 \leq q \leq 2.8)\text{fm}^{-1}$ , the dominant component is M9 where the maximum values is  $10^{-4}$  and  $(1.9)\text{fm}^{-1}$  for form factors and momentum transfer values respectively.

Figure (8) compares the total magnetic form factor between the Valence model (Vm), shown in red line, and the Valence model with core polarization (Vm+Cp), shown in blue line. It is clear from the peaks in the figure that the core effect is very small, because the form factor in our work is transverse.

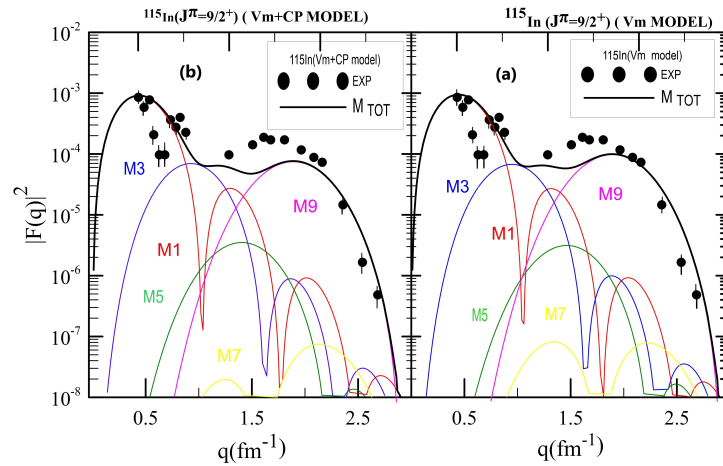


**Figure 7.** The transverse magnetic form factor for  $^{115}\text{In}(J^\pi = \frac{9}{2}^+)$ . The experiment's findings are based on Reference [12].

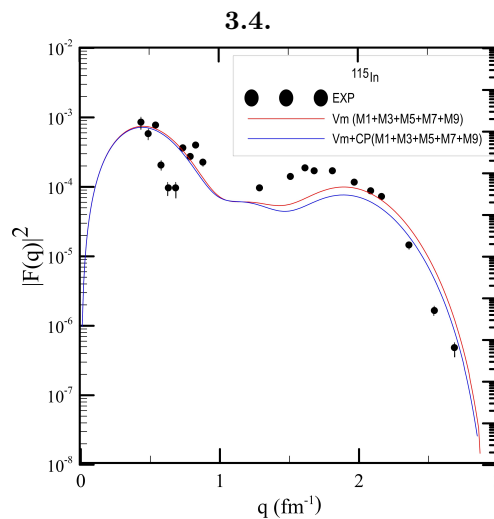


**Figure 8.** Demonstrates compare between Vm and Vm+CP models for  $^{115}\text{In}(J^\pi = \frac{9}{2}^+)$ .

#### 4. CONCLUSIONS

We calculated The magnetic form factors for electron scattering from deformed nuclei (odd-A) in this work. The  $V_m$  and  $V_m$  with  $CP$  Models With  $W0,ho$  and  $glekpn$  as effect interaction and  $Skx&wsn&ho$  as potential describe transversal form factors of  $^{51}\text{V}$ ,  $^{59}\text{Co}$  and  $^{93}\text{Nb}$ ,  $^{115}\text{In}$  well with experimental data.

#### ORCID

Sajad A. Khasain, <https://orcid.org/0000-0003-0000-0000>; Khalid S. Jassim, <https://orcid.org/0000-0002-5990-3277>

#### REFERENCES

- [1] P. Sarriguren, D. Merino, O. Moreno, E. M. de Guerra, D. Kadrev, A. Antonov, and M. Gaidarov, Physical Review C 99, 034325 (2019). <https://doi.org/10.1103/PhysRevC.99.034325>
- [2] R. R. Roy and B. P. Nigam, Nuclear physics: theory and experiment (Wiley, 1967).
- [3] B. Brown, A. Arima, and J. McGrory, Nuclear Physics A 277, 77 (1977). [https://doi.org/10.1016/0375-9474\(77\)90263-9](https://doi.org/10.1016/0375-9474(77)90263-9)
- [4] B. Brown and W. Rae, Nuclear Data Sheets 120, 115 (2014). <https://doi.org/10.1016/j.nds.2014.07.022>
- [5] K. S. Jassim, Physica Scripta 86, 035202 (2012). <https://doi.org/10.1088/0031-8949/86/03/035202>
- [6] X. Pan, Y.-T. Zou, H.-M. Liu, B. He, X.-H. Li, X.-J. Wu, and Z. Zhang, Chinese Physics C 45, 124104 (2021). <https://doi.org/10.1088/1674-1137/ac2421>

- [7] K. S. Jassim, A. A. Al-Sammarrae, F. I. Sharrad, and H. A. Kassim, Physical Review C 89, 014304 (2014). <https://doi.org/10.1103/PhysRevC.89.014304>
- [8] T. de Forest Jr and J. D. Walecka, Advances in Physics 15, 1 (1966). <https://doi.org/10.1080/00018736600101254>
- [9] N. F. Mott, Proceedings of the Royal Society of London. Series A, Containing Papers of a Mathematical and Physical Character 124, 425 (1929). <https://doi.org/10.1098/rspa.1929.0127>
- [10] F. Sharrad, A. Hamoudi, R. Radhi, and H. Abdullah, Journal of the National Science Foundation of Sri Lanka 41 (2013). <http://doi.org/10.4038/jnsfsr.v41i3.6053>
- [11] W. Richter, M. Van der Merwe, R. Julies, and B. Brown, Nuclear Physics A 577, 585 (1994). [https://doi.org/10.1016/0375-9474\(94\)90934-2](https://doi.org/10.1016/0375-9474(94)90934-2)
- [12] T. W. Donnelly and I. Sick, Reviews of modern physics 56, 461 (1984). <https://doi.org/10.1103/RevModPhys.56.461>
- [13] K. Arita, A. Enomoto, S. Oguro, Y. Mizuno, T. Nakazato, S. Ohsawa, T. Saito, T. Terasawa, and Y. Torizuka, Physical Review C 23, 1482 (1981). <https://doi.org/10.1103/PhysRevC.23.1482>
- [14] S. Platchkov, J. Cavedon, J. Clemens, B. Frois, D. Goutte, M. Huet, P. Leconte, X.-H. Phan, S. Williamson, I. Sick, et al., Physics Letters B 131, 301 (1983). [https://doi.org/10.1016/0370-2693\(83\)90503-8](https://doi.org/10.1016/0370-2693(83)90503-8)
- [15] S. Platchkov, J. Bellicard, J. Cavedon, B. Frois, D. Goutte, M. Huet, P. Leconte, P. Xuan-Ho, P. de Witt Huberts, L. Lapikas, et al., Physical Review C 25, 2318 (1982). <https://doi.org/10.1103/PhysRevC.25.2318>
- [16] H. De Vries, G. Van Niftrik, and L. Lapikas, Physics Letters B 33, 403 (1970). [https://doi.org/10.1016/0370-2693\(70\)90615-5](https://doi.org/10.1016/0370-2693(70)90615-5)
- [17] R. York and G. Peterson, Physical Review C 19, 574 (1979). <https://doi.org/10.1103/PhysRevC.19.574>

**МАГНІТНІ ФОРМ-ФАКТОРИ ДЛЯ ДЕЯКИХ ЯДЕР  $^{51}\text{V}$ ,  $^{59}\text{Co}$ ,  $^{93}\text{Nb}$ ,  $^{115}\text{In}$   
ЗА ВИКОРИСТАННЯМ ВАЛЕНТНОСТІ З МОДЕЛЯМИ ПОЛЯРИЗАЦІЙНИХ  
ЕФЕКТІВ ЯДРА ТА БЕЗ МОДЕЛЕЙ**

**Саджад А. Хасейн, Халід С. Джасім**

*Факультет фізики, Коледж навчання фундаментальним наукам, Університет Бабилона, 51002 Бабилон, Ірак*  
Форм-фактор магнітного розсіювання електронів із  $g_{\text{leqn}}$ ,  $d3f7$ , ho моделює простір для ядер  $^{51}\text{V}$ ,  $^{59}\text{Co}$ ,  $^{93}\text{Nb}$ ,  $^{115}\text{In}$  обговорюється з ефектами поляризації ядра (CP) і без них. Розрахунки виконуються за допомогою коду NuShellX@MUS. Радіальну хвильову функцію для одночастинкових матричних елементів було розраховано за допомогою потенціалів Скірма-Хартрі Фока (SKX), Вуда-Саксона (WS) і гармонійного осцилятора (HO). Модель валентності (Vm), використана в цих розрахунках для розрахунку форм-факторів з ефектами поляризації ядра. Результати добре узгоджуються з наявними експериментальними даними.

**Ключові слова:** розсіювання електронів; поперечний форм-фактор